590. *The Properties of Freshly Formed Surfaces. Part X. A New Contracting Liquid-jet Technique for the Study of Soluble Films at Small Surface Ages.*

By C. C. Addison and T. A. Elliott.

A new liquid-jet method is described which enables the simultaneous measurements of surface tension and surface age to be made over time ranges not hitherto accessible. A quantitative study of the following aspects is presented : (*a*) application to pure liquids or ideal solutions of constant surface tension ; (*b*) application to the study of dynamic surface tensions of aqueous solutions ; (*c*) factors (such as surface expansion) which influence the range of applicability of the method.

Investigations on the rates of formation of soluble films at fresh surfaces described in previous parts of this series have shown that the times required for the establishment of equilibrium between the surface and bulk solution may vary from 10^{-3} sec. to several minutes, depending upon the nature and concentration of the solute. Over the major portion of this time range, experimental techniques for the simultaneous recording of time and surface tension are already available ; *e.g.*, in the 0·005—0·1 sec. range, the vibrating-jet technique (Part I, *J.*, 1943, 535) may be applied, and in the time range extending beyond about 2 seconds several methods, including the vertical-plate method (Part VII, *J.*, 1948, 930) and the hanging-drop method (Part VI, *J.*, 1946, 579) are suitable. In general, the time ranges which can be studied by available techniques fall into two clear groups which do not overlap, and there are consequently two time ranges over which the measurement of dynamic tensions has not yet been possible, *viz.*, (*a*) the 0·1—2 sec. range, and (*b*) time ranges below 0·005 sec.

It has now been found possible to determine the surface tension from the dimensions of a vertical non-vibrating jet of liquid ; and we now present a quantitative study of such jets and describe the limiting conditions under which the method may be employed.

When a liquid flows vertically from a circular horizontal orifice it assumes the shape shown in Fig. 1. The contraction of the jet becomes more pronounced as the rate of flow of liquid is reduced, but at a constant flow rate the shape of the jet is determined by the surface tension also. If water or an aqueous solution of high surface tension be considered to give the jet represented by the full lines in Fig. 1, decrease in surface tension of the solution results in a change in shape of jet to that shown by the broken lines *C* and *D*. Therefore, under pre-determined experimental conditions, the horizontal radius of the jet at a given distance from the orifice is a measure of the surface tension of the solution at that position. From the equation of the jet, the age of the surface at that point can also be determined, so that a range of dynamic tensions for any given solution is available from the dimensions of a single jet. As distance from the orifice increases, the radius of the jet is influenced to a lesser extent by changes in surface tension, and when the jet is not contracting appreciably this approach is no longer possible. However, when the jet strikes a solid barrier (*S*, Fig. 1) standing waves are obtained on the jet in the neighbourhood of the barrier. Experiments by Satterly (*Trans. Roy. Soc. Canada*, 1935, **29**, 105) on water jets

indicate that surface tensions may be determined also from the dimensions of these waves. Clear waves are formed only in the lower portion of the jet which is suffering no appreciable contraction. The upper limit of surface age may be increased by lowering the barrier, so that, by a combination of the two methods of measurement, surface tensions are available over the length of the jet.

With regard to time range (*b*), the rapid decrease in tension which occurs, for example, in aqueous solutions of short-chain alcohols on issue from the orifice is not reflected immediately by a corresponding decrease in jet radius, so that the effect of tension changes which may be complete in 10^{-4}—10^{-3} sec. is still apparent at much longer times. The influence of factors, such as added ions, on the rate of adsorption of such short-chain solutes may now be studied qualitatively, and there appears to be no reason why the technique should not be developed to permit quantitative studies of these rapid adsorption rates.

FIG. 1.

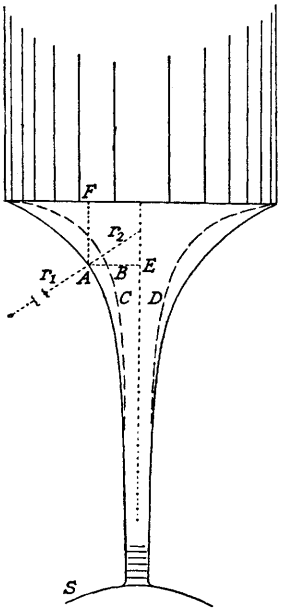

FIG. 2.

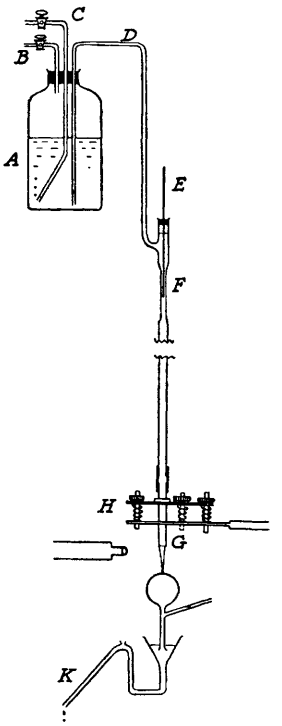

FIG. 2(*a*).

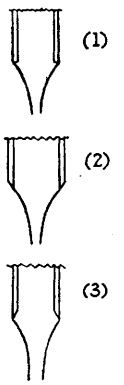

The experiments described in Parts VIII and IX (*J.*, 1948, 936, 943) have shown that expansion of a soluble film may alter the surface tension either by diminishing the surface excess or by modifying the surface activity of the adsorbed molecules. Calculations given below (Section III) show that the jet has an expanding surface, and that the rate of expansion is considerably in excess of the rates which are available by drop methods or in trough experiments using movable barriers. This technique is therefore of additional significance in that it provides a further method for the study of the expansion of soluble films.

Of the various ways referred to above in which the jet technique may be applied, this paper is restricted to a consideration of the measurement of tension from the dimensions of the jet. Other aspects will be considered in later papers.

EXPERIMENTAL.

Apparatus.—The aqueous solution (normally 8—12 l.) was contained in a stoppered 20-l. reservoir *A* (Fig. 2). The reservoir air space was connected to a water-pump *via* tube *B*, to enable the syphon tube *D* to be filled by suction. Tube *C* could be opened to the atmosphere, and when liquid was flowing through *D* to the orifice, tap *B* was closed, and air entered the reservoir through the capillary tube *C* to maintain a constant head of liquid. The air then entered the liquid as a stream of fine bubbles giving minimum agitation of the liquid surface in the reservoir, and prevented the pulsing which arose when wider tubes were used.

The rate of flow of liquid to the orifice was controlled by a valve, comprising a glass rod E (0·35 cm. diam.) which could be moved in tube F (with approx. 0·02 cm. clearance) over a distance of 15 cm. The lower end of F was sealed to a glass tube 150 cm. long and of diameter similar to that of the orifice tube. The latter was connected by rubber tubing, leaving about 0·2 cm. space to allow movement of the orifice tube during levelling.

Constancy of Flow Rate.—The flow of liquid must be quite steady to avoid fluctuations in the jet, and the accurate determination of the flow rate is also necessary for the calculation of surface tensions. When the reservoir was placed at a short distance above the orifice, and the resistance to liquid flow at the valve was small, the flow rate varied by as much as 2%. As the reservoir was raised and the valve resistance increased, the flow rate became steadier. In these experiments the reservoir was placed at a height of 2 m. above the orifice, and the flow rate was then constant to within 0·2%.

Position of Valve.—In order to obtain a steady jet it is necessary that the flow of liquid should be streamlined. When the liquid entered the wide tube from F, a change in linear velocity occurred. This gave rise to turbulent flow, which did not revert to streamlined flow within a distance of about 60 cm. Hence, if the valve is placed near the orifice the jet is unsteady, and accurate measurement of jet radius is not possible. The valve–orifice distance of 150 cm. employed was sufficient to ensure reversion to streamlined flow.

Levelling the Orifice.—Thc orifice tube G was held in a levelling device H (drawn on a magnified scale in Fig. 2) consisting of two triangular plates (10 cm. sides) separated by springs. The lower plate was clamped in position, and the upper plate could be adjusted to any desired level by means of screws passing through the corners of the plates. Tube G was attached rigidly to the upper plate, but could move freely within a hole (larger than G) in the lower plate. In order that its cross-section shall be circular throughout, the jet must flow symmetrically from the orifice. This can be confirmed readily by observing the jet in two mirrors placed together at an angle of about 80°, and so that it is super-imposed on either of the secondary images. Any deviation from jet symmetry is then immediately apparent.

The Barrier.—The jet stream (usually 4 cm. long) was allowed to impinge on a spherical glass surface, etched to ensure complete wetting. The liquid was collected in the funnel device shown, and the flow rate measured by collecting liquid at the overflow K. The introduction of a barrier into a freely-flowing jet caused the jet to be much steadier, and increased the length of unbroken jet, resulting in a 1—4% increase in flow rate according to the position of the barrier.

Curves relating jet radius (r) to distance from the orifice (h) (not reproduced here) have been obtained without a barrier, and for various barrier positions with a constant head of liquid, and it has been confirmed that the only effect which the presence of the barrier has on the h–r curves [on which equation (3), Section I, is based] is that which arises as a result of the variation in flow rate.

Measurement of Jet Dimensions.—Determination of surface tension at any point on the jet surface also involves accurate measurement of the distance of the point from the orifice, and the jet radius at that point. For this purpose a travelling microscope (object glass of focal length 2 in.) fitted with eyepiece scale was used. The jet was illuminated by a strip-light and a diffuse screen placed directly behind the jet. The jet radius was obtained from the calibrated eyepiece scale, and the distance from the orifice measured by movement of the microscope.

Temperature.—The measurements were carried out at room temperature, which did not vary beyond the limits 17° $\pm$ 1·5° during these experiments. In view of other experimental errors involved, this temperature variation is not significant.

Vibration.—The jet is extremely sensitive to even slight vibration. The apparatus was therefore erected on brackets which were built into the main walls of the building.

Shape of Orifice.—The glass orifice used had a horizontally ground lip as shown in Fig. 2(*a*), orifice (1). The liquid flowed invariably from the outside diameter of the tube. Preliminary experiments with orifices of constant external radius, $R = 0{\cdot}747$ cm., and lips of various widths indicated that the dimensions of the jet (at given flow rate) were not influenced over the measured jet length by the width of the lip, provided that this did not exceed about 0·15 cm. For lips of greater width erratic results were obtained. The standard orifice with which all the following results were obtained had a lip width of 0·14 cm. An orifice of type (2), externally ground to a knife edge and having an internal radius R, gave a jet which had, at the same flow rate, dimensions identical with the jet from orifice (1) except in the immediate neighbourhood of the orifice. Since this work does not involve the study of jet dimensions in this region, it is of advantage to employ the orifice tube having the smaller internal radius, since this extends the range of flow rates available (see Section III). Orifices of type (3) Fig. 2(*a*), ground internally (at various angles) to a knife edge, were found to be quite unsuitable. The internal grinding causes the streamlines to diverge at the orifice, and it has not been possible to interpret such jets quantitatively.

Discussion and Results.

Section I. Ideal Liquid Jets.

The term " ideal " is applied here to jets which flow under conditions of constant surface tension, and the present section is confined to a discussion of these jets. The term therefore applies to jets of all pure liquids, and to solutions of compounds (such as inorganic salts) which have negligible surface activity. The presence of any surface-active solute modifies the behaviour of the jet to a degree which is determined (*inter alia*) by the rate of adsorption; jets of such solutions are termed " non-ideal " and are discussed in Section II.

The stream of liquid flowing from an orifice (Fig. 1) undergoes an initial rapid diminution in radius followed by a more gradual change. The factors controlling this shape include density, viscosity, gravity force, liquid flow rate, and the pressure change set up by the operation of the surface tension at the curved surface of the jet. A complete study of the influence of these

various factors is an exceedingly complex problem in hydrodynamics, and according to Lamb ("Hydrodynamics," Cambridge Univ. Press, 1932, p. 24) "the calculation of the form of the issuing jet presents difficulties which have only been overcome in a few ideal cases of motion in two dimensions." However, since the technique was required for the study of dilute aqueous solutions, it was possible in our treatment to ignore the density and viscosity changes, and we have considered in the first instance only the gravity, flow rate, and tension factors.

Bernouille's theorem applied to a jet in which energy is conserved gives

$$\gamma\left(\frac{1}{r_2}-\frac{1}{r_1}\right)+\frac{V^2}{2}-g(H+h)=0$$

where r_2 and r_1 are the internal and external radii of the jet, and V is the linear velocity at any point distance h below the orifice; γ is the surface tension, and H the head of pressure of liquid above orifice level. Except in the neighbourhood of the orifice and at low flow rates, the external radius r_1 in the vertical plane is large, and $1/r_1$ may be neglected. The value of r_2 may be derived in terms of the horizontal radius r and h, but it is simpler to correct for the difference between r and r_2. Since $V = f/\pi r^2$, then

$$g(H+h)=\gamma/r+f^2/2\pi^2r^4 \quad . \quad . \quad . \quad . \quad . \quad . \quad . \quad . \quad . \quad (1)$$

FIG. 3.

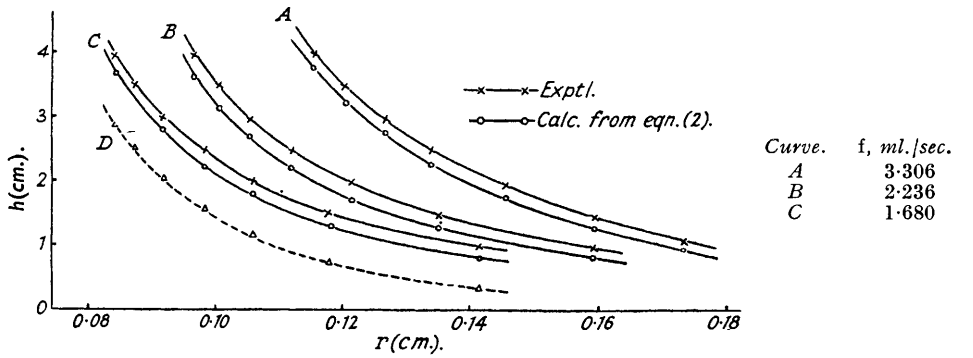

Under optimum conditions for accurate surface-tension measurements, the flow rates are equivalent to H values of the order of 0·1 cm. of water. Since H cannot be determined with the necessary accuracy, it is necessary to eliminate it. The loss in potential energy suffered by unit mass of liquid in falling from the orifice through a distance h is balanced by changes in the curvature and kinetic energies, so that from equation (1)

$$h=\frac{\gamma}{g}\left(\frac{1}{r}-\frac{1}{R}\right)+\frac{f^2}{2\pi^2g}\left(\frac{1}{r^4}-\frac{1}{R^4}\right) \quad . \quad . \quad . \quad . \quad . \quad . \quad . \quad . \quad (2)$$

Curve D, Fig. 3, was calculated for $f = 1{\cdot}680$ ml./sec., the surface-energy term being ignored. Comparison with curve C indicates the order of magnitude of this term. The curves A, B, and C were determined experimentally, and also calculated from equation (2); the two sets of curves are closely similar in shape, but there is a deviation (about 0·2 cm. on the h scale) which varies little with flow rate. This deviation may be attributed chiefly to a horizontal component of velocity and identification of r_2 with r. As change in flow rate does not appreciably alter the discrepancy, it appeared that correction of the first (tension) term rather than the second (flow rate) term was required.

The tension term was therefore modified to $(A\gamma/g)(1/r - 1/R)$; for several flow rates the experimental values of h and r were substituted into the modified equation to determine the values of the empirical factor A. The values of A are plotted against r (Fig. 4); the various A–r curves obtained at different flow rates are seen to combine into a single smooth curve except that slight deviations occur in the case of smaller flow rates and at the high values of r (or small h values) near the orifice, so that over the practical range of f and r the equation of the full curve (Fig. 4) enables A to be expressed in terms of r. The curve is of the general form $A^n =$

$a(r - b)$, and the constants a, b, and n have the values 3·0, 3·59, and 0·0616, respectively. The final form of the equation then becomes

$$h = a(r - b)^{\frac{1}{3}}\frac{\gamma}{g}\left(\frac{1}{r} - \frac{1}{R}\right) + \frac{f^2}{2\pi^2 g}\left(\frac{1}{r^4} - \frac{1}{R^4}\right) \quad . \quad . \quad . \quad . \quad . \quad (3)$$

By employing this equation, the surface tension may be derived from measured values of h, r, and f at any position on the jet for which the correction factors apply (*i.e.*, for h values beyond about 0·3 cm.).

FIG. 4.

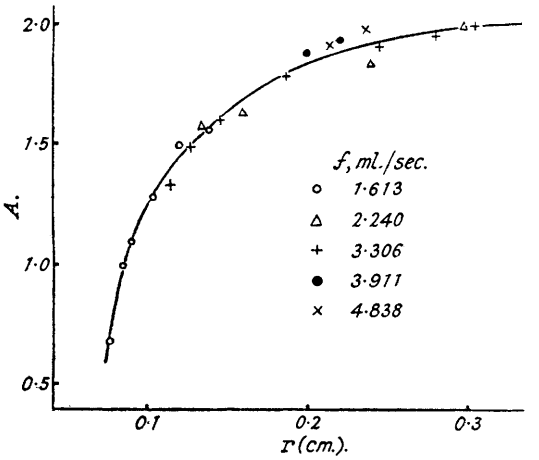

Applicability of Equation (3) *at Low Values of* h.—Over the major portion of the jet, factors other than those considered quantitatively in deriving equation (3) have little influence on the shape of the jet, and are satisfactorily accounted for in the empirical factor A. However, (1) near the orifice the horizontal component of velocity which is then appreciable introduces an additional kinetic energy term into equation (3); surface tensions derived from equation (3) will then appear high; (2) where r_2 is appreciably greater than r (Fig. 13), tensions derived from equation (3) will appear low; (3) neglect of the reciprocal of the external radius r_1 in equation (3) lowers the calculated values of γ, particularly about $h = 0{\cdot}2$ cm. where r_1 passes through a minimum.

FIG. 5.

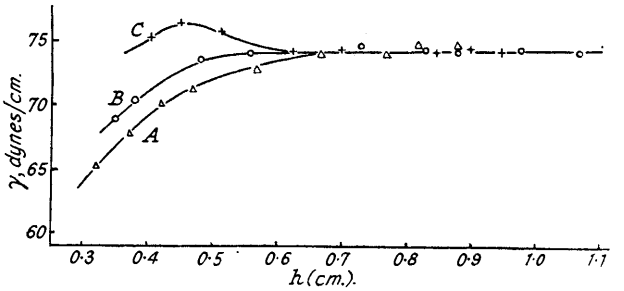

Curve	f, *ml./sec.*
A	2·400
B	3·100
C	*In range* 3·5—5·0

Optimum Flow Rate.—Fig. 5 shows the h–$\gamma_{calc.}$ curves for water. The magnitude of factors (1)—(3) above is a minimum for flow rates between 3·5 and 5·0 ml./sec. At flow rates in excess of this optimum range (*i.e.*, 7—10 ml./sec.) turbulent flow is set up as the liquid leaves the orifice, and high values of surface tension are obtained throughout the jet.

Section II. The Study of Dynamic Surface Tensions.

The different jet shapes given by water and an ideal liquid of lower surface tension are shown qualitatively in Fig. 1. Since the method of derivation of equation (3) is independent of the value of γ, it may be assumed to apply to ideal liquids of any tension value, and measure-

ments reported below justify this assumption. Fig. 6 shows the calculated h–r curves for ideal liquids at four different tensions. If the liquid used is an aqueous solution of a surface-active compound having an equilibrium surface tension of (say) 40 dynes/cm., the surface tension at the moment the liquid leaves the orifice will be near the water value, and the jet will therefore commence in the direction of the ideal water curve (curve A, Fig. 6). As adsorption occurs, the jet will become narrower, and will cut the intermediate ideal liquid curves, approaching the ideal 40 dynes/cm. curve (E, Fig. 6) at an h value which is dependent upon the rate of adsorption. The measured curve for such solutions therefore takes the form represented by the broken curve in Fig. 6. In order to study dynamic surface tensions, it is therefore necessary to devise methods by which the surface age and the tension may be determined at any point on the experimental curve.

FIG. 6.

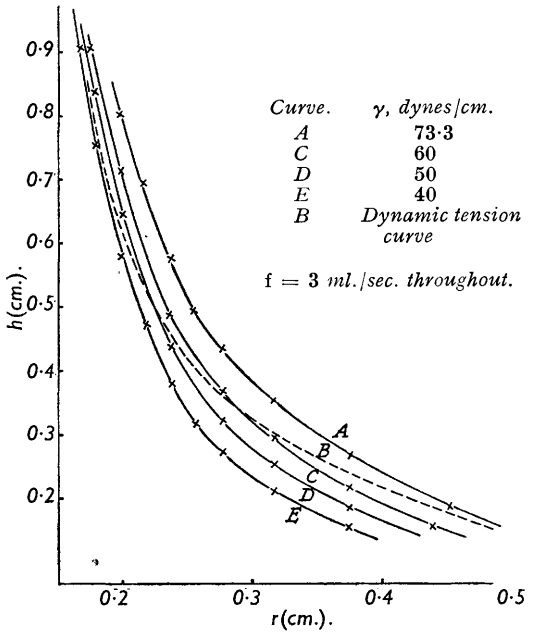

Age of Surface.—If we consider a horizontal lamina of liquid at any point in the jet having thickness δh and radius r, the time (δt) taken by the liquid to travel this distance δh is equal to $\delta h/V$, where V (cm./sec.) is the linear liquid velocity at that point. Now the volume flow rate f (ml./sec.) can be expressed by $\pi r^2 V$, so that $\delta t = \pi r^2 \delta h/f$. The age of the jet at any point at distance h below the orifice can be regarded as the age of the surface at that point provided that there is no appreciable velocity gradient across the jet. At an optimum flow rate of 4 ml./sec. the linear velocity in the orifice tube is 2·25 cm./sec. In view of the low viscosity of dilute aqueous solutions, the velocity gradient across the relatively large orifice tube used will be appreciable only in the neighbourhood of the glass wall of the tube, and will become negligible in the jet where this restriction to flow is removed. The only other source of velocity gradient arises from the contraction of the jet; when the jet assumes cylindrical form this gradient vanishes, and reference to Fig. 6 shows that the rate of contraction is small over the major portion of the jet. Since at $f = 4$ ml./sec. the mean linear velocity in the water jet increases from 2·25 to about 60 cm./sec., the contraction factor is unlikely to give rise to any appreciable deviations from the mean linear velocity. Therefore, the identity of jet age and surface age being assumed,

$$\text{Surface age at point } h = \int_0^h \frac{\pi r^2 \,.\, \mathrm{d}h}{f} = \int_R^r \frac{\pi r^2}{f}\left(\frac{\mathrm{d}h}{\mathrm{d}r}\right)\mathrm{d}r \quad . \quad . \quad . \quad . \quad (4)$$

Alternatively, the time taken to reach point h may be expressed as (volume of jet)/f, and since the volume of the jet is given by $\int_0^h \pi r^2 \,.\, \mathrm{d}h$, the surface age is again that given in equation (4).

Equation (3) gives the necessary relation between r and h, and if γ and f are constant throughout the jet, then

$$\frac{\mathrm{d}h}{\mathrm{d}r} = K_1\left\{\frac{1}{3}\left(\frac{1}{r}-\frac{1}{R}\right)(r-b)^{-\frac{2}{3}} - \frac{(r-b)^{\frac{1}{3}}}{r^2}\right\} - \frac{4K_2}{r^5}$$

where

$$K_1 = a\gamma/g \quad \text{and} \quad K_2 = f^2/2\pi^2 g$$

Now, from equation (4)

$$\text{Surface age} = K_3 \int_R^r \left[(r-b)^{\frac{1}{3}}\left\{\left(\frac{1}{r}-\frac{1}{R}\right)(3br-r^2) - \frac{9(r-b)^2}{7R}\right\} + \frac{4K_2}{K_1 r^2}\right] \quad . \quad . \quad (5)$$

where $K_3 = a\pi\gamma/2fg$. This equation being used, surface ages are recorded in Fig. 7 for a water jet over a range of flow rates, with one curve for an ideal liquid, $\gamma = 40$ dynes/cm. Reduction in the surface tension of the liquid for a given flow rate involves a reduction in surface age

(curves *B* and *C*) but the flow rate is of course the major factor determining surface age. At a sufficiently low flow rate surface ages up to about 0·3 sec. may be obtained (cf. 0·1 sec. maximum with the vibrating jet). In studying dynamic tensions at flow rates so far below the optimum value, equation (3) should be replaced by equation (7) (below), which permits accurate measurement of tension at these lower flow rates. Surface ages have also been determined, by obtaining the volume of the jet graphically, and employing the relation surface age = (jet volume)/*f*. The ages thus obtained are also recorded in Fig. 7, and

FIG. 7.

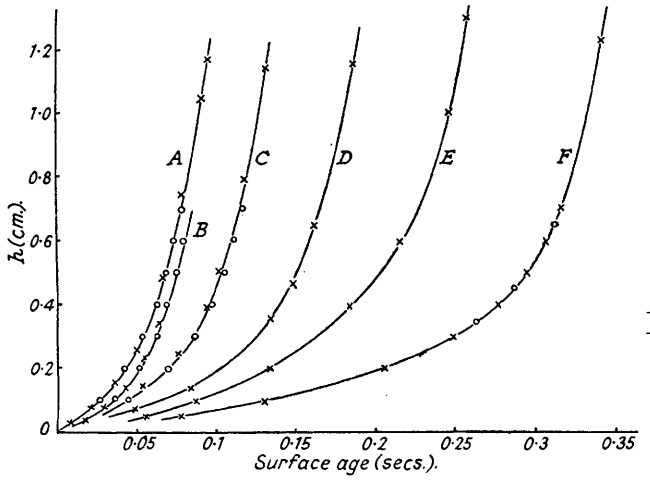

Curve.	*γ, dynes/cm.*	f, *ml./sec.*
A	73·3	5·00
B	40·0	3·00
C	73·3	3·00
D	73·3	2·00
E	73·3	1·50
F	73·3	1·00

— × — × — *Calc.*
— ○ — ○ — *Results obtained graphically.*

show satisfactory agreement with the calculated values. While diffusion to the surface is proceeding in an aqueous solution (*i.e.*, broken curve, Fig. 6) the experimental curve cuts across the ideal curves, and equation (5) is not directly applicable. Equation (4) may then be used, and the volume of the jet determined graphically.

FIG. 8.

Ethyl alcohol solution (equilibrium γ = 50·5 dynes/cm.).

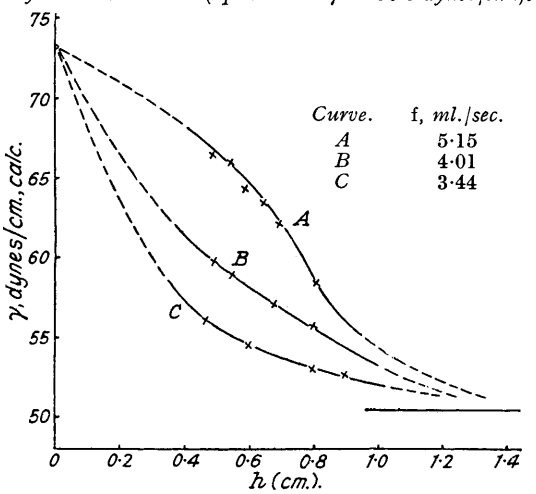

Curve.	f, *ml./sec.*
A	5·15
B	4·01
C	3·44

Measurement of the Surface Tension of Aqueous Solutions.—Aqueous solutions of ethyl alcohol are known from previous work to establish surface equilibrium within 0·004 sec., which is negligible compared with the surface ages recorded in Fig. 7. It was to be expected on these grounds that application of equation (3) to these solutions would give tension values agreeing with the equilibrium values obtained by such standard techniques as the drop-weight method. Fig. 8 shows the results (corrected for the slight density difference) obtained with an 8% solution

of ethyl alcohol at three different flow rates. At high h values the calculated tensions approach the equilibrium (drop-weight) value, but nearer the orifice the discrepancy increases to as much as 16 dynes/cm. The discrepancy increases with increasing flow rate, but for each particular flow rate the γ–h curve is capable of being extrapolated to the water tension at the orifice. Similar effects have been obtained at other concentrations, and with other similar solutes. For example, measurements have been carried out on 0·14 and 0·55% *iso*amyl alcohol solutions (Fig. 9): the same type of γ–h curve is again obtained irrespective of concentration; the curves may be extrapolated back to the water tension at the orifice, but approach the equilibrium tension at a rather higher h value than in the case of ethyl alcohol.

The high calculated tensions indicate that at a given point in the jet the measured radius must be greatly in excess of the radius of the ideal jet at that h value, and the results in Figs. 8 and 9 may be interpreted as follows. A jet of water flowing from an orifice (shown in semi-outline in Fig. 10) can be considered to follow curve NH, while an ideal liquid having $\gamma = 50$ dynes/cm. will follow curve ND at the same flow rate. A solution of ethyl alcohol will have a

FIG. 9.

iso Amyl alcohol solutions.

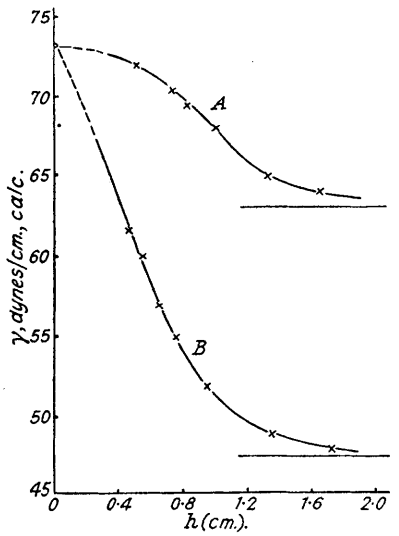

Curve.	*Equilibrium γ, dynes/cm.*	f, *ml./sec.*
A	63·0	3·93
B	47·6	4·07

FIG. 10.

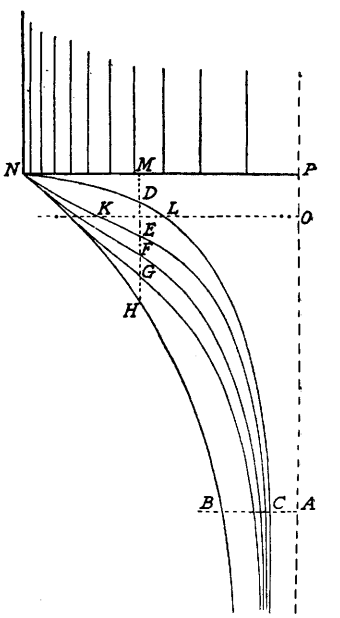

surface tension near the water value at the instant of surface formation at the orifice, and will therefore commence along curve NH. When surface equilibrium is established (say, at point K, curve KE) the radius KO is then considerably in excess of the ideal radius LO. The different shapes of curves NK and NL arise from two factors, now to be discussed.

(1) The energy of unit mass of liquid in the ideal system NL differs from that in the non-ideal system NK. Hence, for a given flow rate f, the energy E_1 in system NL may be expressed, at a sufficient distance PA below the orifice, as

$$E_1 = T_1 - g(PA + H_1) + \gamma_1/r_{AC}$$

where T_1 is the kinetic energy, and H_1 is the head of pressure above the orifice level required to produce the flow rate f. Now, the curvature energy produces a back pressure restricting the flow of liquid, and for any given system, irrespective of whether the tension is constant or changing, there is a characteristic H value required to produce a particular flow rate, and hence a characteristic energy value. Therefore for the water system NH

$$E_2 = T_2 - g(PA + H_2) + \gamma_2/r_{AB}$$

and similar considerations apply to the changing tension systems NE, NF, etc.

In consequence, the ideal equation (3) which is applicable at point L cannot be applied to point K, since although K and L are at the same horizontal level they differ in potential energy. Again, it follows that the changing tension curves can never meet the ideal curve NL; but as distance from the orifice increases, H becomes less significant (*i.e.*, H_1–H_2 becomes negligible) so that the tensions measured by the ideal equation (3) approach the equilibrium value at points distant from the orifice.

(2) The shape of the jet reflects the distribution of energy between the three types : surface, kinetic, and potential energy. A conservative energy system being assumed, the variation in surface energy which occurs as the tension changes modifies the normal distribution of energy between kinetic and potential which occurs in an ideal system.

At the orifice all jets of dilute aqueous solutions will have surface tension near that of water, and a similar initial direction. Any difference in the energy sum for the respective systems, due to variation in head of pressure, will not be appreciable, and variation in adsorption rates will then be reflected in the energy distribution, and consequently in the shape of the curve. To test this, solutions of ethyl, *iso*amyl, and *sec.*-octyl alcohols were prepared. These solutions had the same equilibrium tension of 47·6 dynes/cm., and the flow rate was kept at 4·07 ml./sec. throughout. The calculated tension–h curves are given in Fig. 11, and show that the discrepancies in the calculated tensions increase as the times for surface equilibration (< 0·004,

FIG. 11.

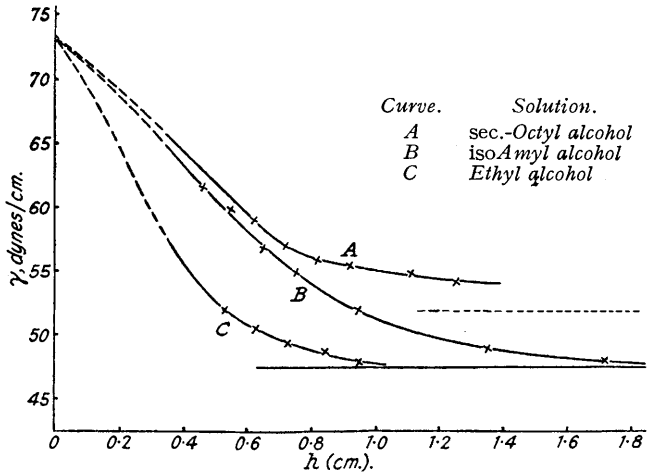

0·012, and 0·045 sec., respectively) increase. The expansion and/or contraction which occurs in the jet surface (discussed in detail below) does not appreciably influence the ethyl and *iso*amyl alcohol tensions; because of surface expansion the surface tension of the *sec.*-octyl alcohol solution cannot fall below 52 dynes/cm., and the apparent tensions level off towards this value.

Hitherto the shortest surface ages recorded have been those measured by the vibrating jet and reported in earlier parts of this series; no method has been described which is capable of recording or reflecting the rapid adsorption which occurs with solutes of chain length below $C_{(5)}$. However, the discrepancies between calculated and true surface tensions recorded for ethyl alcohol solutions in Fig. 11 arise directly from the initial surface diffusion process. In this respect the present method is unique, and may be applied to the study of adsorption at the very short surface ages below the lower limit of the vibrating jet.

Very Short Surface Ages.—In order to determine the time–tension relationship for the ethyl alcohol adsorption process, it would be necessary to measure these quantities over the full curve NKE (Fig. 10) and with particular accuracy in the range NK. Equation (7) (below) permits the calculation of the true (rather than the apparent) tension at any point on this curve. However, the jet shown diagrammatically in Fig. 10 is exaggerated in a vertical direction for clarity, and for the ethyl alcohol system adsorption is complete within a distance of about 0·1 cm. from the orifice. With the measurements at present available it is only possible to set a maximum to the time required to complete the diffusion to the surface. Changes in these times are reflected in the relative distances MD,ME, MF, etc. (Fig. 10), and if the position of MH is so chosen that equilibrium has by then been attained, the times of adsorption should be related to these distances

by a smooth curve. These distances have been measured for the series of solutions given in Table I, and at $f = 4{\cdot}07$ ml./sec.

TABLE I.

Aqueous solution used.	Equilibrium surface tension, dynes/cm.	Time to reach surface equilibrium, secs.	h (cm.) for $r = 0{\cdot}300$.	h (cm.) for $r = 0{\cdot}216$.
Ideal	47·6	Nil	0·317	0·703
10% Ethyl alcohol	47·6	Unknown	0·335	0·710
0·55% *iso*Amyl alcohol	47·6	0·012	0·360	0·750
0·037% *sec.*-Octyl alcohol	47·6	0·045	0·366	0·765
Pure water	—	∞	0·430	0·869

In this table the ideal values are included for comparison, and the water jet is taken to represent the behaviour of a solution requiring an infinite time to establish surface equilibrium. The values of h can be graphed against known times of diffusion. Unfortunately, no diffusion times are yet known for alcohols below C_5, so the actual position of that portion of the graph between the *iso*amyl alcohol and the ideal value is somewhat arbitrary, but the graph indicates that adsorption must be complete within 0·002 sec.

Although the actual adsorption rates are not yet available, the present technique permits

FIG. 12.

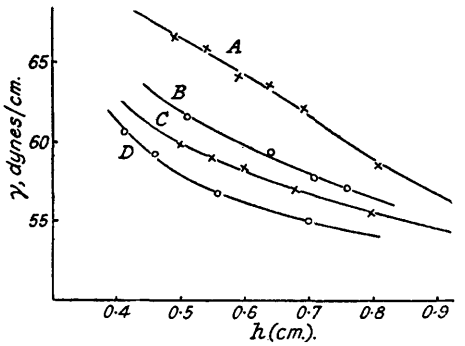

f, *ml./sec.*	*Curve.*	*Solution used.*	γ, *dynes/cm., by drop weight.*
5·15 4·007	*A* *C*	8% *Ethyl alcohol*	50·5
5·00 4·05	*B* *D*	8% *Ethyl alcohol* + 1·8% NaCl	51·4

FIG. 13.

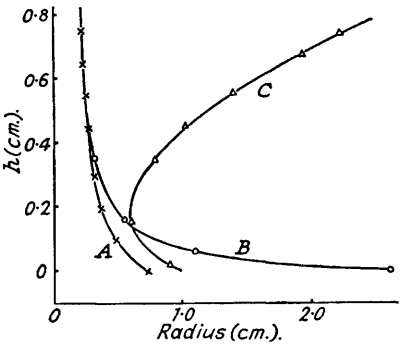

A. Horizontal radius.
B. True internal radius.
C. External radius.

the qualitative study of the influence of added solutes on this adsorption rate. Fig. 12 shows γ–h curves, calculated by equation (3), for ethyl alcohol solutions in the presence of 1·8% of sodium chloride. The apparent tensions are depressed by several dynes/cm. Since the equilibrium tension of the ethyl alcohol solution is increased by about 1 dyne/cm. by the addition of the salt, the actual differences will be greater than those shown in Fig. 12 by this amount. It follows that the rate of adsorption of ethyl alcohol molecules to the surface is increased by the addition of sodium chloride to the solution.

Surface Ages in the Range 0·005—0·4 *Second.*—This time range is approximately that covered by the whole jet, and it is clear from the above that equation (3) is not applicable for the determination of true tensions of aqueous solutions. Three alternative approaches are possible.

(1) *With a water jet as reference.* Consider two jets, one of water and one of an aqueous solution of a surface-active compound, flowing from identical orifices and having the same flow rate f, and select a point on each jet (A and B, respectively) at which the horizontal radius has the same value r. Then the h values of points A and B (h_1 and h_2, respectively) will differ. If $r_{1(a)}$ and $r_{1(b)}$, and $r_{2(a)}$ and $r_{2(b)}$ represent the respective external and internal radii at points A and B, then the sum of the energies of unit mass of liquid at A may be represented as

$$\frac{f^2}{2\pi^2 r^4} + K.E._{\text{Horiz.}} + \gamma_w \left(\frac{1}{r_{2(a)}} - \frac{1}{r_{1(a)}}\right) - g(h_1 + H_1)$$

where γ_w represents the surface tension of water and $K.E._{\text{Horiz.}}$ is the horizontal kinetic energy; a similar expression applies for point B. Measurements made on a number of jets have shown that, except in the region of the orifice, the slope of the h–r curve (dh/dr) is dependent largely on the value of r, and differs only slightly with the surface tension of the solution. Therefore the horizontal component of the velocity may be considered to be equal at A and B. Over the measured portion of the jets (Table II) H is small compared with h. If any slight difference between H_1 and H_2 exists, this difference will be quite negligible, so that energies at A and B may be equated, and if γ_s represents the surface tension at point B, then

$$\Delta hg = \gamma_w \left(\frac{1}{r_{2(a)}} - \frac{1}{r_{1(a)}}\right) - \gamma_s \left(\frac{1}{r_{2(b)}} - \frac{1}{r_{1(b)}}\right) \quad . \quad . \quad . \quad . \quad . \quad . \quad . \quad (6)$$

Now internal radius $$r_2 = r\left\{1 + \left(\frac{dh}{dr}\right)^2\right\}^{\frac{1}{2}} \Big/ \frac{dh}{dr}$$

and external radius $$r_1 = \left\{1 + \left(\frac{dh}{dr}\right)^2\right\}^{3/2} \Big/ \frac{d^2h}{dr^2}$$

The value of dh/dr should be determined separately for each curve, since small variations in the calculated radii influence the tension value to a much greater extent than do similar variations in the $K.E._{\text{Horiz.}}$ term. The values r, Δh, and dh/dr can be obtained directly from the measured h–r curves; if dh/dr is plotted against r, then the value of d^2h/dr^2 can be obtained from the slope of this curve, and since γ_w is constant, the value of γ_s may be calculated from equation (6). The results given in Table II have been calculated from equation (6) by using the same jet measurements as were employed when deriving the high apparent tensions by equation (3) (Figs. 9, 11, and 12).

TABLE II.

Solution used.	h (cm.).	Horizontal radius (cm.).	γ_s, dynes/cm.
Ethyl alcohol + 1·8% NaCl (Drop-wt. γ = 51·4 dynes/cm.)	0·360	0·3010	51·6
	0·410	0·2835	50·5
	0·910	0·2004	50·2
*iso*Amyl alcohol (Drop-wt. γ = 47·6 dynes/cm.)	0·450	0·2730	46·5
	0·650	0·2315	47·4
	0·850	0·2049	48·0
	1·050	0·1894	48·0
	1·150	0·1834	48·0
sec.-Octyl alcohol (Drop-wt. γ = 47·6 dynes/cm., equivalent to 52·0 dynes/cm. when allowance is made for surface expansion)	0·520	0·2568	50·5
	0·720	0·2255	51·5
	0·920	0·2012	52·0
	1·120	0·1866	51·5
	1·320	0·1757	51·5

Equation (6) gives the correct value of the tension, within experimental error, for non-ideal jets, and may therefore be applied directly to the study of adsorption rates over the time range of 0·005—0·4 sec. It is of interest here to record the relative magnitudes of the horizontal, internal, and external radii at different points of the jet, since this relation determines the accuracy with which the various radii must be measured. Fig. 13 shows these values for the 0·55% *iso*amyl alcohol solution (for which calculated tensions are given in Table II). The magnitudes of the ethyl alcohol and *sec.*-octyl alcohol jet radii are similar. The horizontal and true internal radii become almost identical in value as the jet approaches cylindrical form, and over the same h range the external radius becomes so large as to be ultimately negligible.

(2) *With a point of known tension as reference.* The approach given above suffers from the practical disadvantage that it is necessary to measure h–r curves for both the water and the aqueous solution jets at an identical flow rate. Equation (7) below permits calculation of surface tensions from measurements on the jet of alcohol solution alone, and is not restricted to any optimum flow rate range.

The reference point can be determined in two ways: (*a*) If the tension is changing throughout the jet, the reference point can be taken as the point at which the jet strikes a barrier, in which case the tension at that point is available from the dimensions of the waves on the jet. (*b*) If the solution is known to establish equilibrium early in the jet, any point in the lower part of the jet may be taken as reference.

If we now define A on the alcohol solution jet as the reference point of known tension, and

B as the point of unknown tension on the same jet, and designate the various dimensions as follows:

Jet positions.	Horizontal radius.	External radius.	Internal radius.	Surface tension.	Distance from orifice.	Slope of h–r curve.
A	r_a	$r_{1(a)}$	$r_{2(a)}$	γ_a	h_1	$(\mathrm{d}h/\mathrm{d}r)_a$
B	r_b	$r_{1(b)}$	$r_{2(b)}$	γ_b	h_2	$(\mathrm{d}h/\mathrm{d}r)_b$

then the total energy at each point is given by the energy expression in (1) above. Since the horizontal radii at A and B now differ, it is not possible to eliminate either the vertical or the horizontal kinetic energy terms in equating energies at A and B, and thus

$$\Delta K.E._{\text{Vert.}} + \Delta K.E._{\text{Horiz.}} + \Delta \text{ Curvature energy} = \Delta hg$$

The horizontal component of the velocity must diminish towards the centre of the jet, but if $V_{\text{Vert.}}$ represents the mean vertical velocity then a suitable approximation is given by the ratio $V_{\text{Vert.}}/(\mathrm{d}h/\mathrm{d}r)$.

If we assume that $$K.E._{\text{Horiz.}} = \frac{f^2}{2\pi^2 r^4(\mathrm{d}h/\mathrm{d}r)^2}$$

then the equation

$$\frac{f^2}{2\pi^2}\left(\frac{1}{r_a^4} - \frac{1}{r_b^4} + \frac{1}{r_a^4(\mathrm{d}h/\mathrm{d}r)_a^2} - \frac{1}{r_b^4(\mathrm{d}h/\mathrm{d}r)_b^2}\right) + \gamma_a\left(\frac{1}{r_{2(a)}} - \frac{1}{r_{1(a)}}\right) - \gamma_b\left(\frac{1}{r_{2(b)}} - \frac{1}{r_{1(b)}}\right) = g(h_1 - h_2) \quad . \quad . \quad (7)$$

contains only readily measurable terms.

Equation (7) has been tested on jets of pure water and an ethyl alcohol solution, and typical results are given in Table III. The calculated tensions are true within experimental error.

TABLE III.

Liquid tested.	(1.) h, cm.	(2.) $K.E._{\text{Horiz.}}$ (ergs).	(3.) $K.E._{\text{Vert.}}$ (ergs).	(4.) γ (dynes/cm.).
(*a*) 8% Ethyl alcohol + 1·8% NaCl (Equilibrium surface tension = 51·4 dynes/cm.)	0·460	12·18	157·8	52·7
	0·560	9·95	233·2	51·6
	0·610	8·17	274·6	50·5
	0·660	7·12	306·2	52·3
	0·710	6·19	348·6	51·3
	0·810	4·92	434·0	51·7
	0·911 *	3·70	515·0	51·4
(*b*) Pure water (γ = 73·3 dynes/cm.)	0·500	11·6	125·2	72·7
	0·600	10·1	182·7	73·7
	0·700	8·6	246·7	74·0
	0·800	7·1	316·0	73·6
	0·900 *	6·07	394·0	73·3

* Reference points.

Cols. (2) and (3) show the relative magnitudes of the two kinetic-energy terms. With further refinement of the experimental technique it should be possible to apply this equation up to the orifice; the $K.E._{\text{Horiz.}}$ term would then become of major significance, and would require more accurate determination.

(3) *With the orifice as reference.* The method now described, which is a modification of (2) above, finds wide application in the study of very dilute solutions, where adsorption rates are slower. Under these conditions the tension at the freshly formed surface, and $\mathrm{d}h/\mathrm{d}r$ at the orifice, will be almost exactly that of water; the orifice can then be used as a reference point. It is then necessary, in calculating tensions at a given point in the jet, to use the jet dimensions at that point only, and the (*a*) and (*b*) suffixes (equation 7) need no longer be used. Equation (7) then simplifies to

$$hg = \frac{f^2}{2\pi^2 r^4}\left(1 + \frac{1}{(\mathrm{d}h/\mathrm{d}r)^2}\right) + \gamma_s\left(\frac{1}{r_2} - \frac{1}{r_1}\right) - K_f \quad . \quad . \quad . \quad . \quad . \quad (8)$$

where the various dimensions are defined as in equation (7), and

$$K_f = \frac{f^2}{2\pi^2 R^4}\left(1 + \frac{1}{(\mathrm{d}h/\mathrm{d}r)_R^2}\right) + \gamma_w\left(\frac{1}{R_2} - \frac{1}{R_1}\right) \quad . \quad . \quad . \quad . \quad . \quad (9)$$

All the dimensions in equation (9) are referred to the jet at the point where it meets the orifice, and K_f is a characteristic of the orifice, depending only on the flow rate. The value of K_f may be determined by direct measurement, but is most readily obtained, for solutes having slower adsorption rates, by applying equation (8) to water jets over a range of flow rates, when the value of K_f is found to vary almost linearly with flow rate. With the orifice used, $K_f = -134{\cdot}5$ for $f = 4{\cdot}07$ ml./sec. With use of this value, equation (8) has been applied to the jet obtained with 0·037% *sec.*-octyl alcohol (see Table II). The results are given in Table IV and are in satisfactory agreement, for present purposes, with the true value of 52·0 dynes/cm.

TABLE IV.

h, cm.	0·420	0·620	0·820	0·920	1·020	1·120
Surface tension (dynes/cm.)	51·5	53·3	53·1	52·7	51·3	51·4

Section III. Factors Governing the Range of Applicability of the Method.

(1) *Expansion or Contraction of the Surface.*—Measurements of the change in surface area of unit volume of liquid which occurs as this unit volume proceeds down the jet, have shown that in all cases a surface contraction occurs during the initial 0·2 cm. of jet, and is followed by a fairly rapid expansion which extends throughout the remainder of the jet. For solutions (of,

FIG. 14.

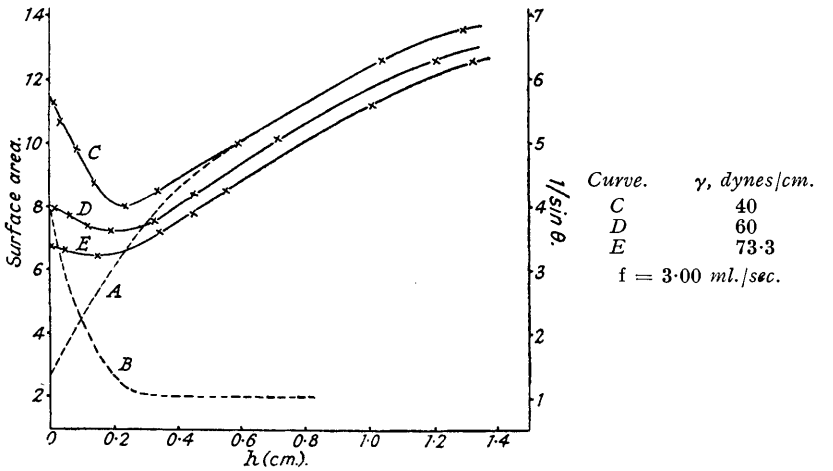

e.g., ethyl and *iso*amyl alcohol) in which surface equilibrium is established rapidly, calculation has confirmed that the rates of change of surface area involved are insufficient to influence the equilibrium surface tension. Where slower rates of adsorption are concerned, surface expansion may cause the tensions at the jet surface to be appreciably different from the stationary surface values.

If we first consider a thin horizontal lamina of liquid to be in the form of a cylinder, then the surface area (for unit volume) is given by $2/r$. The change in area due to this effect alone is shown in Fig. 14 by curve *A*. In fact, the lamina is a frustrum of a cone, mean radius r, and the surface area depends also upon the angle of the cone. If the slope of the h–r curve, dh/dr, is $\tan\theta$, then the change in area due to change in θ is given by $1/\sin\theta$ (curve *B*, Fig. 14). The resultant area changes, expressed as $2/r \sin\theta$, are shown by curve *C*. Although the variation in surface area beyond $h = ca.$ 0·2 cm. is almost independent of surface tension, the initial contraction of the jet is less pronounced as tension increases, and is only slight in the case of pure water. Fig. 15 shows the influence of flow rate on the surface area; the major increases in area are observed at low flow rates. This does not imply that surface expansion is more rapid, since differing surface ages are involved; by means of the information in Fig. 7, the area–h curves in Fig. 15 can be transcribed into area–time curves, when it may be shown that the actual rate of surface expansion (cm.²/sec.) is almost independent of flow rate. This fact, taken in conjunction with Fig. 14, implies that the rate of surface expansion is primarily determined by the size of the orifice, and is little influenced by surface tension or flow rate.

It may be deduced from Figs. 14 and 15 that an area of 1 cm.^{2} will expand to about 15 cm.^{2} in 1 second. This rate is considerably in excess of that available by other methods. In the drop-weight method (Part VIII, *J.*, 1948, 936) the surface area is approximately doubled in 1 second, and in trough–movable barrier experiments surface expansion in excess of this latter rate results in the formation of surface ripples. This jet technique is therefore of value in that it enables the influence of surface expansion to be studied in systems which show no tension change

FIG. 15.

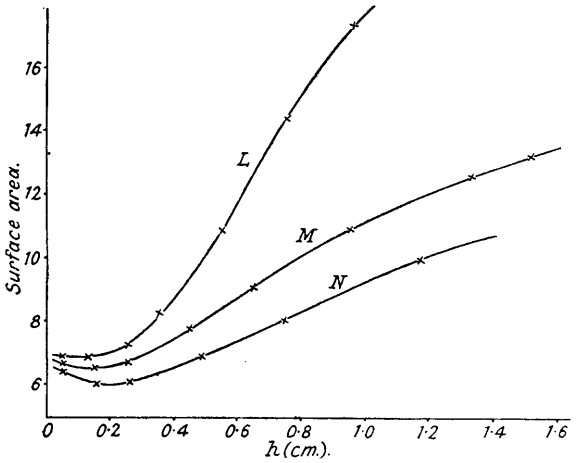

Curve.	f, *ml./sec.*
L	1·00
M	3·00
N	5·00

γ = 73·3 *dynes/cm.*

at the slower rates of expansion available by other methods. For example, the surface tension of a *sec.*-octyl alcohol solution, as measured by the drop-weight method, is not influenced by rate of formation of the drop, but is raised to the extent of 4·4 dynes/cm. above the equilibrium value at the expanding jet surface. The rate of adsorption to a stationary surface is known from vibrating-jet measurements (Part III, *J.*, 1944, 477). From the corresponding h–r curve the area–h relation may be deduced (as in Figs. 14 and 15); this may be transcribed into an area–time curve, from which the rate of surface expansion may be obtained. By using this inform-

FIG. 16.

0·037% sec.-*Octyl alcohol solution.*

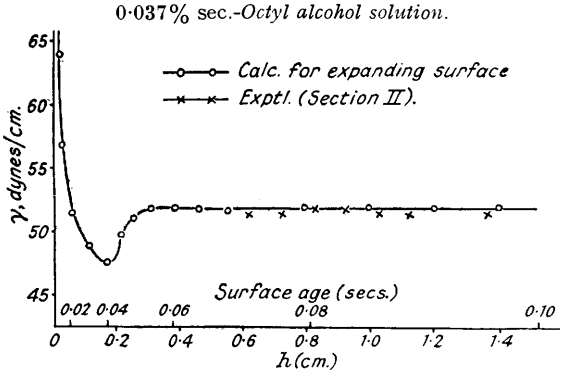

ation, and the stepwise approach described in Part VIII (*loc. cit.*), the influence of surface expansion has been calculated for the 0·037% *sec.*-octyl alcohol solution. The tensions are plotted against time and h in Fig. 16. Owing to the initial contraction of the surface, the tension falls to the equilibrium value of 47·6 dynes/cm. in 0·040 sec. (compare 0·045 sec. at a stationary surface). The surface then changes from contraction to expansion; the surface excess consequently diminishes (*i.e.*, the tension increases) until the rate of adsorption is balanced by the rate of surface expansion. This balance occurs at a tension value of 52·0 dynes/cm.; thereafter the tension is maintained at this figure, and this (rather than the equilibrium tension) is the value determined by the methods described in Section II.

(2) *Accuracy of Tension Measurement.*—Assuming that f, h, R, and r are measured with appropriate accuracy, the degree of error in the measurement of the surface tension at any point in the jet is dependent upon the extent to which the radius is influenced by tension changes (distance A–B Fig. 1). A–B has been deduced from " ideal " h–r curves for water and a liquid of surface tension 40 dynes/cm., and is plotted against distance from the orifice in Fig. 17 for several flow rates. Since all jets originate from the rim of the orifice, A–B is initially zero. Fig. 17 indicates that A–B passes through a maximum (which becomes greater as the flow rate diminishes) and that when the jet approximates to cylindrical form (*i.e.*, at h values beyond about 2 cm.) the jet radius varies little with change in tension. The A–B values are recorded in terms of eyepiece scale divisions (where 1 division = $3{\cdot}977 \times 10^{-3}$ cm.) and represent variations of 4—35% of the actual radius of the water jet. Under the experimental conditions employed, it was possible to determine radius values with an accuracy of 0·1 division. On this basis, the values listed in Table V indicate the maximum errors arising from measurement of radius, and further refinement of experimental technique would reduce these errors.

TABLE V.

	Experimental error dynes/cm. Flow rates, ml./sec.			
h, cm.	1.	3.	5.	8.
0·1	0·11	0·13	0·16	0·22
0·3	0·11	0·15	0·22	0·28
0·5	0·19	0·31	0·36	0·42
0·7	0·35	0·44	0·51	0·60
1·0	0·60	0·70	0·78	0·84
1·5	1·36	1·36	1·36	1·36

The degree of accuracy in the measurement of tension is thus sufficiently great to enable the technique to be directly applicable to the study of dynamic tensions and surface diffusion

FIG. 17.

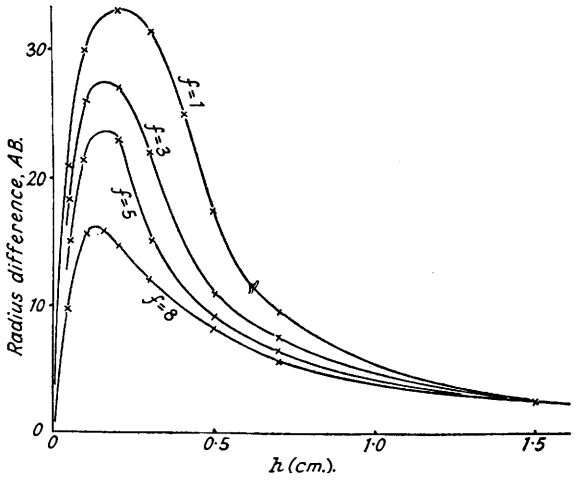

processes; the method fulfils an entirely different function from the many more accurate methods designed for measurements at static surfaces, and no grounds exist for comparison.

(3) *Critical Flow Rate for Jet Formation.*—Under any given experimental conditions there is a minimum liquid flow rate below which the jet collapses (termed the " critical flow rate " to avoid confusion with other minima referred to in this paper), and this sets the lower limit to the range of flow rates available experimentally. This lower limit varies with surface tension and jet radius, so that the factors governing its operation merit more detailed consideration. On the basis of the energy equations [*e.g.*, equation (8)] only, it would seem possible to reduce the flow rate to values almost infinitely small without collapse of the jet. However, experiments show that jet collapse may occur, with solutions of low surface tension, at flow rates as high as 10 ml./sec., and it appears that for jet stability the area/volume ratio of the contracting portion of the jet must not exceed that of the liquid suspended on the orifice after jet collapse.

When the flow rate is diminished, the ratio, area/volume of jet liquid, is increased. Fig. 18 shows the variation in area/volume ratio with flow rate for water, and for an ideal liquid assumed to have a surface tension of 40 dynes/cm. throughout the jet. As flow rate varies, the change in area/volume ratio occurs largely in the upper contracting portion of the jet. When the jet collapses, the break occurs approximately at the position where the jet assumes cylindrical form. The selection of this position is somewhat arbitrary; curves *AB* and *CD* (Fig. 18) have been calculated for that portion of the jet up to 0·7 cm. from the orifice. This represents a suitable measured mean, and the positions of the curves are not altered appreciably by variations of $\pm 0{\cdot}1$ cm. in the adopted h value. When the jet breaks, the lower cylindrical portion falls away in the form of drops; and the upper contracting portion remains suspended on the orifice. A study of the shape of this suspended liquid immediately after collapse, and the influence of surface tension on this shape, lies outside the scope of this investigation, but measurements of minimum flow rates indicate that the limits of area/volume ratio lie approximately along the line *BD* (Fig. 18) and point *D* therefore represents the minimum flow rate available for a water jet. Since for the liquid of low surface tension the area/volume ratio is greater (curve *AB*) the maximum ratio for jet stability is reached at a higher flow rate (point B, Fig. 18). The non-ideal alcohol solutions discussed in Section II will give area/volume curves lying between *AB* and *CD*, but will be governed by the same principles.

FIG. 18.

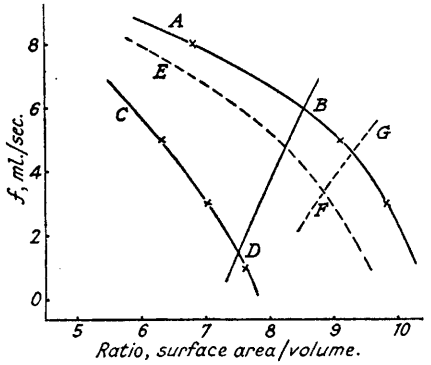

Curve.	*γ, dynes/cm.*
AB	40
CD	73·3

FIG. 19.

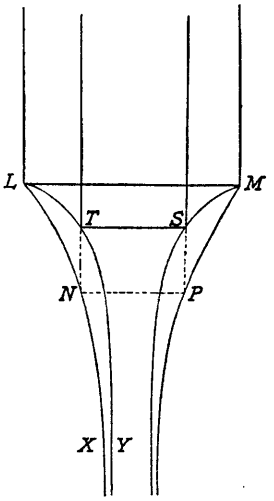

Slight reduction in orifice radius is found to cause a considerable decrease in the critical flow rate. The effect is illustrated in Fig. 18. By appropriate reduction in R the curve *AB* moves to some position *EF*. Since the volume of liquid suspended on the orifice after jet collapse is reduced, its area/volume ratio is increased, and the limiting curve *BD* moves to position *FG*. In consequence, the minimum available flow rate is decreased from *B* to *F*. Considering this radius factor alone, the restrictions in the use of the technique which arise as a result of the operation of the critical flow rate effect are less significant with narrow orifices. However, the accuracy with which tensions may be measured diminishes with decreasing R, and it was these considerations which led to the selection of the orifice radius used as a suitable mean between these two conflicting effects. Some minimum flow-rate values have been measured for three orifices of slightly different radii, employing various solutions of *iso*amyl alcohol, and are recorded in Table VI.

TABLE VI.

Internal radius of orifice tube (cm.).	Critical flow rate, ml./sec. $\gamma = 73{\cdot}5$ dynes/cm.	$\gamma = 62{\cdot}5$ dynes/cm.	$\gamma = 53{\cdot}5$ dynes/cm.	$\gamma = 46$ dynes/cm.
0·7471	2·3	4·0	5·8	10·6
0·6021	1·3	1·6	2·5	4·4
0·5794	—	—	1·2	1·9

(4) *Significance of Orifice Radius.*—Since the derivation of equation (3) was independent of the magnitude of R, for a given flow rate and tension there should be only one possible ideal jet, the orifice radius determining merely the position at which the jet commences on the h range. Thus if LNX (Fig. 19) be considered to be the water jet from orifice LM, water flowing from a smaller orifice NP should follow the same curve NX, and similar considerations apply for larger orifices. To confirm this, equation (3) was applied, without change in the constants involved, to measure h and r values for a water jet from an orifice of 0·579 cm. radius, and the calculated tensions for two flow rates are given in Table VII. For a flow rate of 2·202 ml./sec. the results

TABLE VII.

(*a*) f = 2·202 ml./sec.	h, cm.	0·300	0·435	0·585		
	γ, dynes/cm.	74·2	76·0	75·2		
(*b*) f = 4·141 ml./sec.	h, cm.	0·450	0·530	0·740	0·840	1·050
	γ, dynes/cm.	84·0	82·2	78·0	77·1	74·8

differ from the true value by little more than the experimental error. However, it appears that when liquid is delivered from a smaller orifice turbulent flow commences at a lower flow rate, and thus for this orifice the maximum in the optimum flow rate range is about 2·5 ml./sec. (compared with 5·0 ml./sec. for R = 0·747 cm.). Above this f value turbulent flow gives rise to high calculated γ values, as was observed (Fig. 5) for the larger radius.

Therefore for the measurement of the surface tension of a pure liquid, the available upper limit of R is determined by the critical flow rate; the lower limit is determined only by practical considerations, *i.e.*, the accuracy with which r can be measured. However, for the measurement of differences in surface tension R should be as large as possible. If an ideal liquid of low surface tension flows from orifice LM (Fig. 19) its shape can be represented (relative to the water curve LNX) by the curve LTY. It has been shown above that the form of the jet is independent of R, and this can be considered to hold true whatever the value of the surface tension. Thus the liquid of low tension flowing from the smaller orifice would have the form TY. In order to compare the two jets from orifice NP, curve TY must be displaced vertically downwards by a distance TN. The horizontal distance between the two curves at any point will then clearly be smaller than that obtained with the larger orifice.

THE UNIVERSITY, NOTTINGHAM.

[*Received, May 11th,* 1949.]